[redacted]

Copy 2
RM E57D17

NACA RM E57D17

NACA

# RESEARCH MEMORANDUM

## EFFECTS OF FREE-STREAM REYNOLDS NUMBER, ENGINE INSTALLATION, AND MODEL SCALE ON STABILITY CHARACTERISTICS OF A TRANSLATING-SPIKE INLET AT MACH 2.0

By Norman T. Musial and David Bowditch

Lewis Flight Propulsion Laboratory
Cleveland, Ohio

CLASSIFICATION CHANGE

To Unclassified
By authority of CAN #7761, H.G. Myers
Changed by M. Ruda Date 12-10-58

CLASSIFIED DOCUMENT

This material contains information affecting the National Defense of the United States within the meaning of the espionage laws, Title 18, U.S.C., Secs. 793 and 794, the transmission or revelation of which in any manner to an unauthorized person is prohibited by law.

NATIONAL ADVISORY COMMITTEE
FOR AERONAUTICS

WASHINGTON

November 13, 1957

FILE COPY
To be returned to the files of the National Advisory Committee for Aeronautics Washington, D. C.

[redacted]

[redacted]

NATIONAL ADVISORY COMMITTEE FOR AERONAUTICS

RESEARCH MEMORANDUM

# EFFECTS OF FREE-STREAM REYNOLDS NUMBER, ENGINE INSTALLATION, AND MODEL SCALE ON STABILITY CHARACTERISTICS OF A TRANSLATING-SPIKE INLET AT MACH 2.0

By Norman T. Musial and David Bowditch

## SUMMARY

The effect of free-stream Reynolds number, engine installation, and model scale on inlet stability limits and on the amplitude and frequency of buzz are presented. The data were taken at a free-stream Mach number of 2.0 and angles of attack from $0^{\circ}$ to $6^{\circ}$.

Subcritical stability was not affected when the Reynolds number (based on cowl diameter at the lip) was reduced from $9.0\times10^{6}$ to $2.4\times10^{6}$ by decreasing the free-stream tunnel pressure. However, a further reduction in Reynolds number to $1.71\times10^{6}$ resulted in an increase of subcritical stability. Although the frequency of buzz appeared to be independent of Reynolds number, buzz amplitude varied with Reynolds number. Values of amplitude and frequency increased at a faster rate and reached a higher value for the engine than for the full-scale cold pipe. The subcritical stability obtained both with the engine and with a quarter-scale cold-flow inlet was greater than that obtained with the full-scale cold pipe.

## INTRODUCTION

Pulsing of supersonic inlets has long been observed, and several theories have been advanced to explain this aerodynamic phenomenon (refs. 1 to 3). The pulsing characteristics and inlet performance are usually obtained from small-scale models utilizing an exit plug in place of the engine. These results are applied directly to the full-scale engine configuration.

As noted in reference 4, tests on a full-scale inlet at Mach 1.8 and 2.0 indicated that the stability limits of the inlet were increased by replacing the exit plug used for cold-flow testing with a J34 turbojet

[redacted]

engine. In further cold-flow tests made on the same inlet (ref. 5) inlet stability limits were obtained for three different choking stations downstream of the inlet. The stability limits obtained with the engine were not precisely duplicated with any of the cold-pipe designs; however, the data indicate the possibility of approximating the engine if the correct cold-pipe configuration is used.

An investigation was made in the Lewis 10- by 10-foot supersonic wind tunnel with a turbojet engine of more advanced design than the J34 engine of reference 4 in combination with an axially symmetric inlet that had a blunt lip and a translating spike. The investigation of the full-scale inlet was conducted both with the engine installed and with an exit plug (ref. 6). Cold-flow Reynolds number was varied by changing the tunnel pressure altitude from 49,000 to 85,000 feet. The full-scale cold-pipe results are compared in this report with the quarter-scale results of reference 7.

Presented herein are the effect of free-stream Reynolds number, engine installation, and model scale on inlet stability limits and on the amplitude and frequency of buzz. Data are presented at a free-stream Mach number of 2.0 and angles of attack from $0^\circ$ to $6^\circ$.

## SYMBOLS

The following symbols are used in this report:

| | |
|---|---|
| $A$ | flow area |
| $m$ | mass flow, slugs/sec |
| $P$ | total pressure, lb/sq ft |
| $p$ | static pressure, lb/sq ft |
| $\frac{p_{2,max} - p_{2,min}}{P_0}$ | amplitude ratio as a percent of tunnel total pressure |
| Re | Reynolds number, based on inlet cowl diameter (full-scale inlet cowl diameter equals 2.56 ft) |
| $\theta_l$ | cowl-lip-position parameter defined as angle between axis of spike and line joining cone apex and cowl lip |

Subscripts:

| | |
|---|---|
| max | maximum |
| min | minimum |
| 0 | free stream |
| 1 | cowl inlet |
| 2 | diffuser discharge or compressor inlet, station 81.4 |

## APPARATUS AND PROCEDURE

The model consisted of an inlet located ahead of either a cold pipe or a turbojet engine as shown in figure 1. Relative size of the installation in the 10- by 10-foot supersonic tunnel is indicated by the photograph of figure 2.

The inlet had a remotely actuated translating $25^{\circ}$ half-angle spike, with a blunt-lip cowl. Three subinlets were located in the diffuser and, for the data in this report, were operated full open and choked. A complete description of the blunt lip and subinlets is given in reference 6. Variation of inlet flow area is given in figure 3.

The engine had a seventeen-stage axial-flow compressor and a three-stage turbine. The stators in the first seven stages of the compressor were variable; they were positioned by sensing engine speed and compressor-inlet temperature. The variable nozzle is scheduled by power level position and biased by exhaust gas temperature.

Dynamic pressure transducers were located at several longitudinal stations in the engine and cold-pipe configurations (fig. 1) in order to detect amplitude and frequency of pulsation. The traces from the pressure pickups were recorded on optical and pen-type instruments. The natural frequency of the optical recorder was about 100 cycles per second, and the natural frequency of the pen type was about 50 cycles per second.

Minimum stability curves for the cold-flow configuration were obtained in the following manner: For each cowl-lip-position parameter $\theta_l$, the plug was moved to reduce mass flow until the inlet terminal shock, as observed by schlieren and dynamic pressure pickups, just started to oscillate. The plug position was noted, and the plug was retracted, then extended as closely as possible to the previous position without actually putting the inlet into buzz. For the engine configuration, inlet mass flow was decreased by reducing engine speed until a pulse amplitude, as a specified percent of tunnel total pressure, was indicated on the recorder.

Free-stream Reynolds number was changed by varying the tunnel pressure level. Table I gives the range covered for zero angle of attack as well as the corresponding pressure altitude of the tunnel and the pressure altitude for the same Reynolds number at standard-day temperatures and Mach 2.0. The total temperature in the tunnel was maintained at about 545° R for all the data.

The subcritical inlet mass flows for the cold-pipe configuration were calculated by means of the static pressure and area at the exit plug. Subcritical mass flows for the engine configuration were determined by using the engine airflow curve. Mass flows thus obtained are believed to be accurate to ±2 percent.

## RESULTS AND DISCUSSION

### Free-Stream Reynolds Number Effect

The effect of free-stream Reynolds number on the inlet stability of the full-scale cold-pipe configuration is presented in figure 4. No appreciable difference in stability limits was apparent between Reynolds numbers of $9.0\times10^6$ and $2.4\times10^6$ at zero angle of attack. Although not as complete a range of data was taken, no noticeable differences were found at higher angles of attack for the same Reynolds number range.

A reduction in Reynolds number to about $1.71\times10^6$ had the effect of increasing subcritical stability for all angles of attack. The increase in stability occurred at low values of cowl-lip-position parameter $\theta_l$ for zero angle of attack (fig. 4(a)) and at high values of $\theta_l$ for angles of 3° and 6° (figs. 4(b) and (c)). This effect occurs at a tunnel pressure altitude of about 85,000 feet (table I). The corresponding flight pressure altitude for the same Reynolds number at standard-day conditions and Mach 2.0 is about 76,000 feet.

Schlieren observations at zero angle of attack, a Reynolds number of $2.4\times10^6$, and a $\theta_l$ value of 37.75° showed that instability was apparently "triggered" by the impingement of the vortex sheet on the cowl lip while, at a higher value of $\theta_l$ (40.7°), vortex-sheet passage over the cowl lip had no effect. The oblique shock off the cone falls inside the cowl lip above a $\theta_l$ of about 41°. When the Reynolds number was reduced to $1.71\times10^6$, vortex-sheet impingement on or over the cowl lip at a $\theta_l$ value of 37.75° had no effect on stability.

The supercritical flow indicated in figure 4 varies with $\theta_l$. This variation is the result of increasing spillage by the oblique shock as $\theta_l$ is decreased. Spillage caused by the blunt lip prevents the mass-flow ratio from reaching unity.

Data were taken while going into buzz for two values of $\theta_l$ and at zero angle of attack to determine the buzz amplitude and frequency for the cold pipe. These data are given in figure 5 for $\theta_l$ values of $37.75^\circ$ and $40^\circ$. While the mass-flow ratios at which buzz is initiated did not change for a reduction of Reynolds number to $2.4\times10^6$ and a $\theta_l$ value of $37.75^\circ$, the buzz amplitude did vary (fig. 5(a)). As the Reynolds number was reduced to $1.71\times10^6$, no buzz was encountered down to a mass-flow ratio of about 0.49, where buzz started abruptly and reached a high value very quickly. Visual observation (at $Re \approx 2\times10^6$) showed that the terminal shock fluttered as the vortex sheet passed over the cowl lip and continued to do so until the vortex sheet was well inside the cowl. However, the flutter was not strong enough to be sensed through the pressure pickups and was not considered a buzz condition.

Buzz, at a higher value of $\theta_l$ (fig. 5(b)), started at about the same mass-flow ratio for both Reynolds numbers ($2.4\times10^6$ and $1.71\times10^6$). The amplitude of buzz measured for both numbers increased at about the same rate.

Frequency of buzz at all Reynolds numbers and for both values of $\theta_l$ ($37.75^\circ$ and $40^\circ$) increased rapidly and reached a maximum of about 10 cycles per second. Closed-end-pipe theory indicates a fundamental frequency of about 10 cycles per second for the full-scale exit-plug configuration.

Pulsing traces obtained with the cold pipe are shown in figure 6. Although the pulse trace was nearly sinusoidal for low pulse amplitude (fig. 6(a)), presence of a third harmonic can be seen on the trace at the diffuser discharge. The modification by the third harmonic at the diffuser discharge became more evident when the amplitude of buzz was further increased (fig. 6(b)). At the lower Reynolds number of $1.71\times10^6$ (fig. 6(c)), buzz started initially with the predominant frequency modified by the third harmonic.

The shape of the pressure wave for both Reynolds numbers was modified farther back in the nacelle and seemed to approach a square wave at the exit-plug station. The change in shape of the pressure oscillation from station to station could possibly be due to a phase shift between the first and third harmonic evident at the diffuser discharge. It is interesting to note that, for these data, the amplitude of buzz increased with increasing nacelle station. Similar data, previously obtained from another full-scale nacelle (ref. 8), indicated no consistent trend of amplitude increase or decrease with increasing nacelle station.

## Model Scale

A comparison of the quarter-scale-model stability limits with those of the full-scale model is made in figure 7 at angles of attack of $0^\circ$ to $6^\circ$. At all angles of attack, the quarter-scale model had more subcritical stability than the full-scale inlet and reached complete stability at a lower value of $\theta_l$.

Buzz information was obtained on the quarter-scale model (ref. 7) by putting the inlet into buzz and by defining the buzz limit as the point at which buzz stopped when the mass-flow ratio was increased. Hysteresis effects, in comparing the data to the full-scale model, are believed to be small; however, any hysteresis effect present will increase the difference in stability limits. Also, the quarter-scale model did not have subinlets, whereas the full-scale configuration has three that were full open for the stability data. The removal of the low-energy air through the subinlets possibly had an effect on buzz limits.

The physical dimensions of the quarter-scale model to the diffuser discharge (station 2) are accurately proportioned to those of the full-scale configuration (table II). However, the length (and consequently the volume) to the choke point of the full-scale model exceeds that of the corresponding scaled-up value calculated from the quarter-scale configuration by about nine feet or about four inlet diameters. Although the data are limited in application and should be recognized as such, quarter-scale complete stability is reached at a lower value of $\theta_l$ than that of the full-scale configuration. This effect of length and volume agrees with a similar trend noted with a full-scale configuration in reference 5.

In figure 8, a comparison is made of the amplitude and the frequency of quarter-scale and full-scale configurations for a $\theta_l$ value of $37.75^\circ$ at about the same Reynolds number. Initially, the pressure amplitude increases at about the same rate for both configurations; however, the pressure amplitude values for the full-scale configuration are less than the quarter-scale values at low mass-flow ratios. The frequency of the quarter-scale configuration rises to a much greater value than that of the full-scale configuration and approximates the fundamental closed-end-pipe theory of about 65 cycles per second.

## Effect of Engine on Stability

Reference 4 indicates that a J34 engine had a stabilizing effect on subcritical inlet stability, compared with an exit-plug configuration. This effect was also observed with the turbojet engine tested in this investigation, as shown by the results in figure 9. The engine inlet configuration at all angles of attack had more subcritical stability and reached complete stability at a lower value of $\theta_l$ than the exit-plug configuration.

A comparison of the inlet buzz frequency and amplitude for the exit-plug configuration and for the engine configuration at zero angle of attack is presented in figure 10. The amplitude and frequency of buzz at the compressor inlet increased at a faster rate and reached higher values with the engine than with the cold pipe. Although these data are at slightly different values of $\theta_l$, it is felt that the trends are valid. These values of frequency and amplitude were obtained with pen-type recording instrumentation.

Damping of buzz through the engine is quite similar to the J34 engine data reported in reference 8. Oscillations in terms of absolute pressure were amplified through the compressor (fig. 11(a)); however, for windmilling conditions, the engine damped pressure oscillations. Since the absolute pressure increased, total amplitude as a percent of local pressure was greatly reduced by the compressor (fig. 11(b)). The same trend was noted for the J34 engine.

The oscillations were completely damped by the time the flow reached the turbine discharge station (fig. 11(b)), whereas it was observed that, for the J34 engine, pressure oscillations existed downstream of the turbine. For the present investigation, frequency of pulsation was not changed in going through the compressor (fig. 11(c)). Because the time constant of the engine is about 1 to 2 seconds, the amplitude of the engine-speed oscillation would be negligible at a buzz frequency of 14 to 24 cycles per second.

Pulsation traces are shown in figure 12 for operating points A, B, and C of figure 11(c). The data at the compressor face were obtained with the pen-type recorder, whereas data at the other stations were obtained with an optical type that had a different recording speed. A frequency of about 100 cycles per second, which might be associated with compressor rotation, was superimposed on the predominant frequency of the compressor discharge.

## SUMMARY OF RESULTS

The following results were observed in an investigation on the effects of free-stream Reynolds number, engine installation, and model scale on the stability characteristics of a translating-spike inlet at Mach 2.0:

1. Subcritical stability increased when Reynolds number (based on inlet capture diameter) was reduced below $2.4\times10^6$ by lowering tunnel static pressure.

2. Frequency of buzz appeared to be independent of Reynolds number, but buzz amplitude was affected by Reynolds number.

3. Subcritical stability of the full-scale inlet at angles of attack from $0^{\circ}$ to $6^{\circ}$ was greater with the engine than with the exit plug.

4. The amplitude and frequency of buzz increased at a faster rate and reached a higher value when the turbojet engine was used instead of an exit plug.

5. Subcritical stability of the quarter-scale inlet was greater at all angles of attack tested than that obtained with the full-scale inlet.

Lewis Flight Propulsion Laboratory
National Advisory Committee for Aeronautics
Cleveland, Ohio, June 7, 1957

## REFERENCES

1. Trimpi, Robert L.: A Theory for Stability and Buzz Pulsation Amplitude in Ram Jets and an Experimental Investigation Including Scale Effects. NACA Rep. 1265, 1956. (Supersedes NACA RM L53G28.)

2. Sterbentz, William H., and Evvard, John C.: Criterions for Prediction and Control of Ram-Jet Flow Pulsations. NACA TN 3506, 1955. (Supersedes NACA RM E51C27.)

3. Mirels, Harold: Acoustic Analysis of Ram-Jet Buzz. NACA TN 3574, 1955.

4. Beheim, Milton A., and Englert, Gerald W.: Effects of a J34 Turbojet Engine on Supersonic Diffuser Performance. NACA RM E55I21, 1956.

5. Musial, Norman T.: Comparison of Effect of a Turbojet Engine and Three Cold-Flow Configurations on the Stability of a Full-Scale Supersonic Inlet. NACA RM E56K23, 1957.

6. Hearth, Donald P., Anderson, Bernhard H., and Dryer, Murray: Performance Comparison at Mach Numbers 1.8 and 2.0 of Full-Scale and Quarter-Scale Translating Spike Inlets. NACA RM E57D16, 1957.

7. Anderson, Arthur A., and Weinstein, Maynard I.: Aerodynamic Performance of Several Techniques for Spike-Position Control of a Blunt-Lip Nose Inlet Having Internal Contraction at Mach Number of 0.63 and 1.5 to 2.0. NACA RM E57D15, 1957.

8. Beke, Andrew, Englert, Gerald, and Beheim, Milton: Effect of an Adjustable Supersonic Inlet on the Performance Up to Mach Number 2.0 of a J34 Turbojet Engine. NACA RM E55I27, 1956.

[redacted]

TABLE I. - REYNOLDS NUMBER RANGE

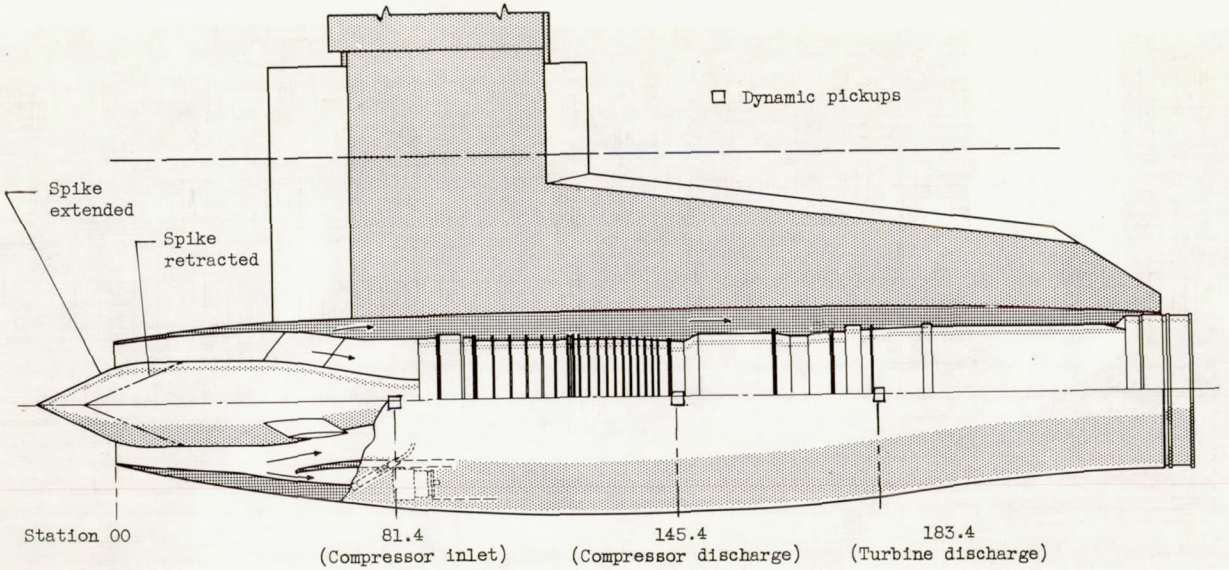
| Reynolds number | Tunnel total pressure, lb/sq ft abs | Tunnel pressure altitude, ft | Flight pressure altitude, ft (a) |
|---|---|---|---|
| $9.0\times10^6$ | 1950 | $49\times10^3$ | $42\times10^3$ |
| 6.7 | 1450 | 55 | 48 |
| 3.58 | 775 | 69 | 61 |
| 2.4 | 520 | 77 | 69 |
| 1.71 | 370 | 85 | 76.5 |

[a]Standard-day conditions; Mach 2.0.

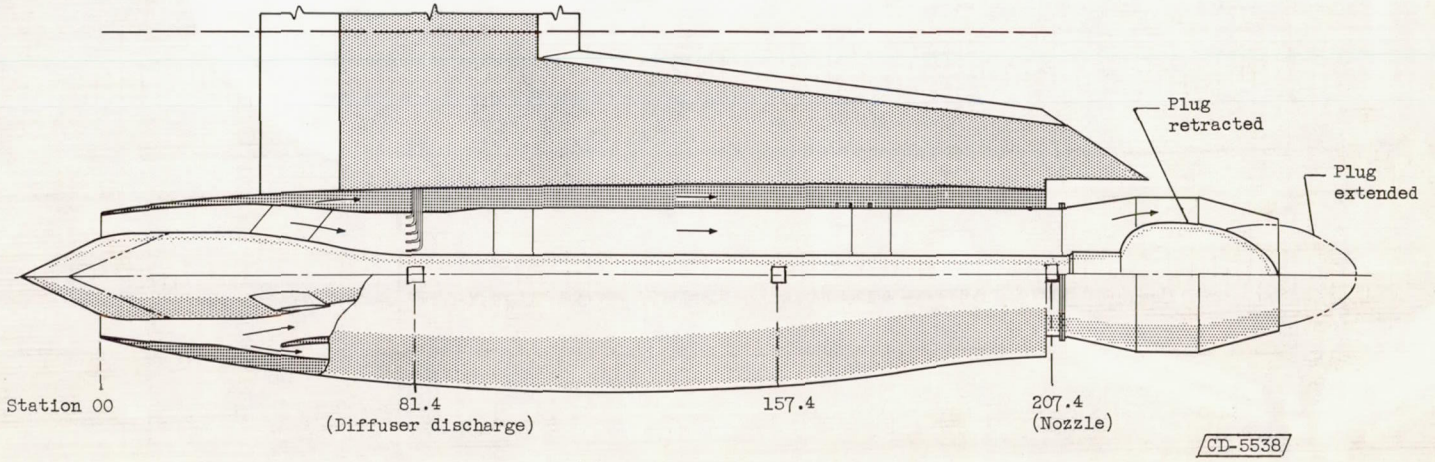
TABLE II. - LENGTHS AND VOLUMES OF COLD-PIPE CONFIGURATIONS

| | Quarter-scale model | Theoretical full-scale measurements calculated from quarter-scale model | Actual full-scale model |
|---|---|---|---|
| Length to compressor face, ft | 1.77 | 7.08 | 7.08 |
| Length to choke point, ft | 4.15 | 16.6 | 25.5 |
| Volume to compressor face, cu ft | .43 | 28.5 | 28.5 |
| Volume to choke point, cu ft | 1.18 | 76.5 | ≈107.0 |

[redacted]




(a) Engine.




(b) Cold pipe.

Figure 1. - Schematic diagram of nacelle configurations.

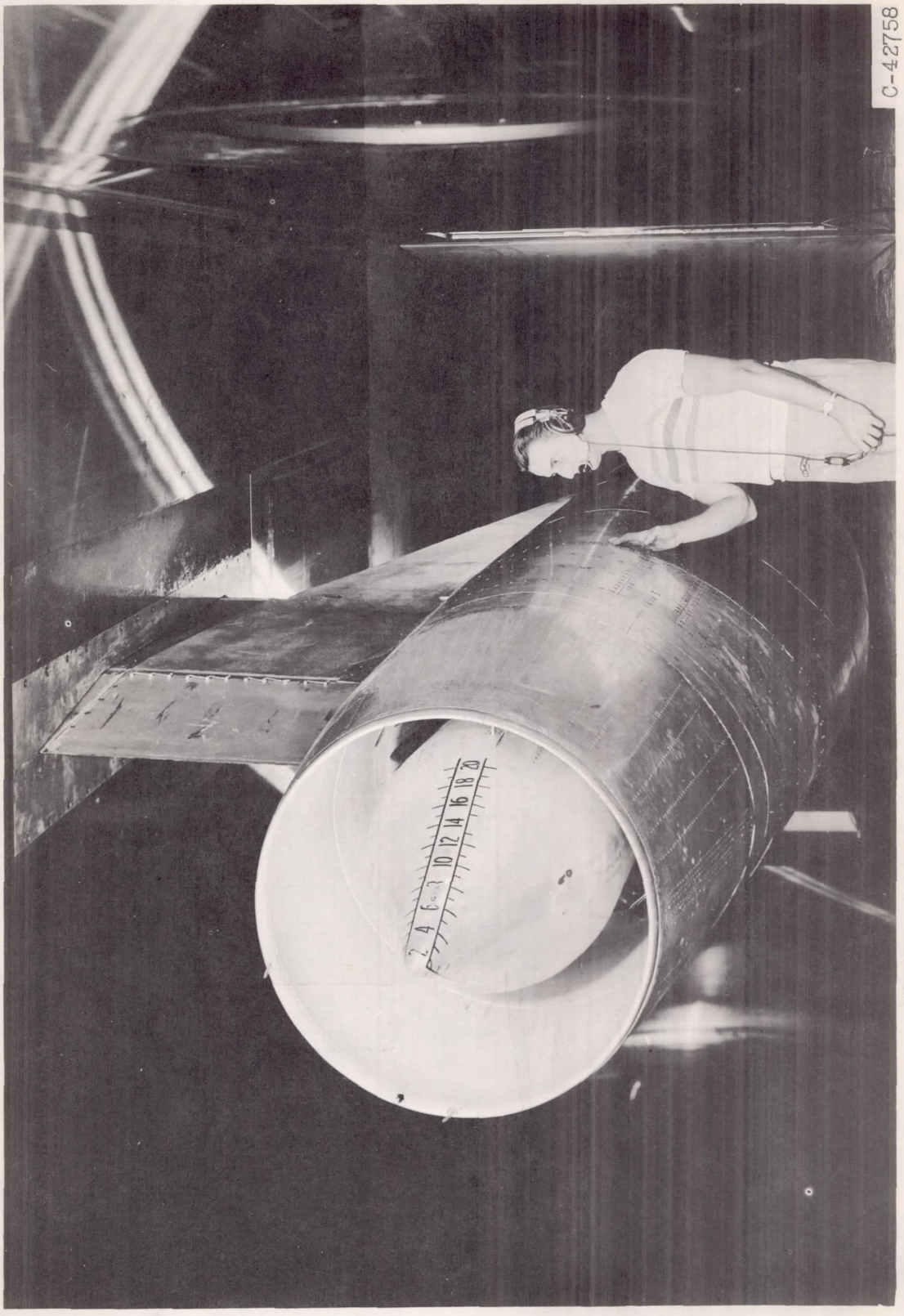



Figure 2. - Nacelle in tunnel.

[redacted]

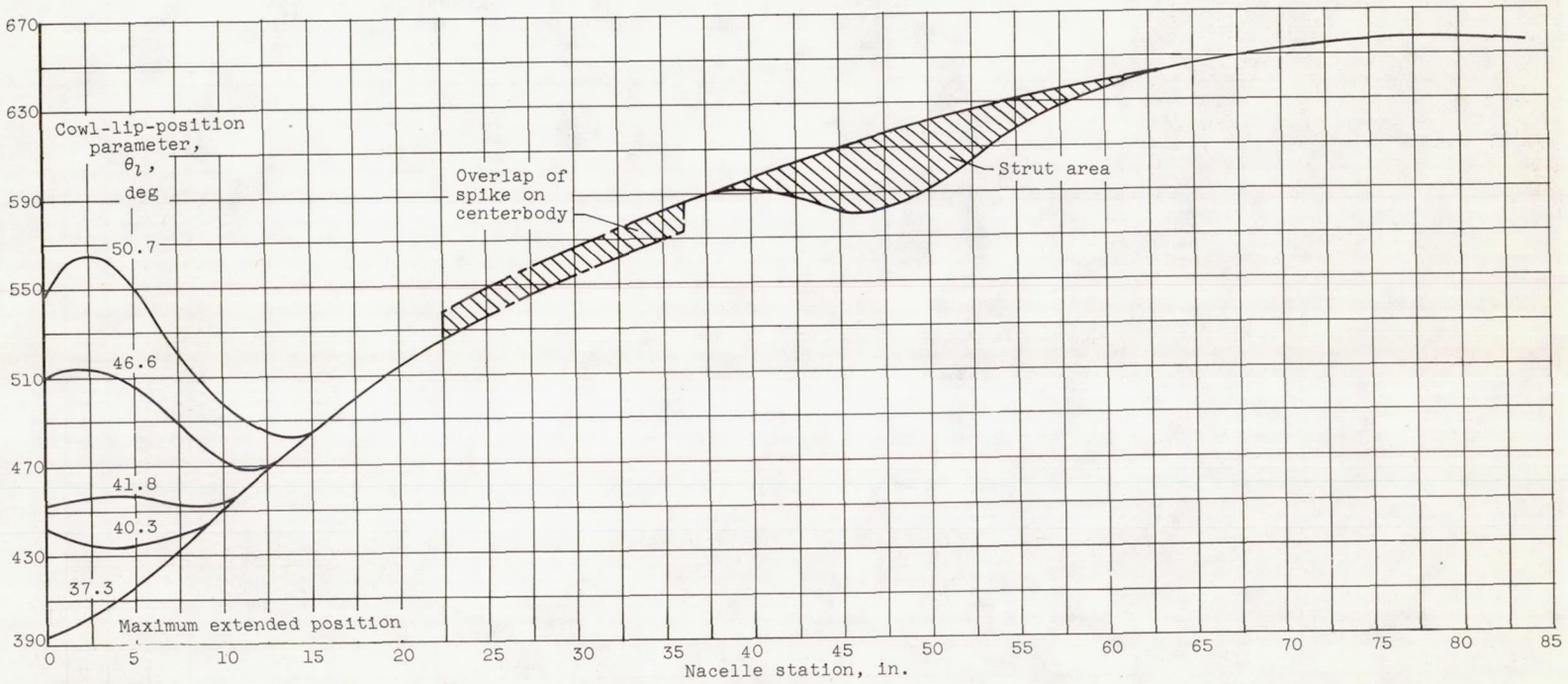
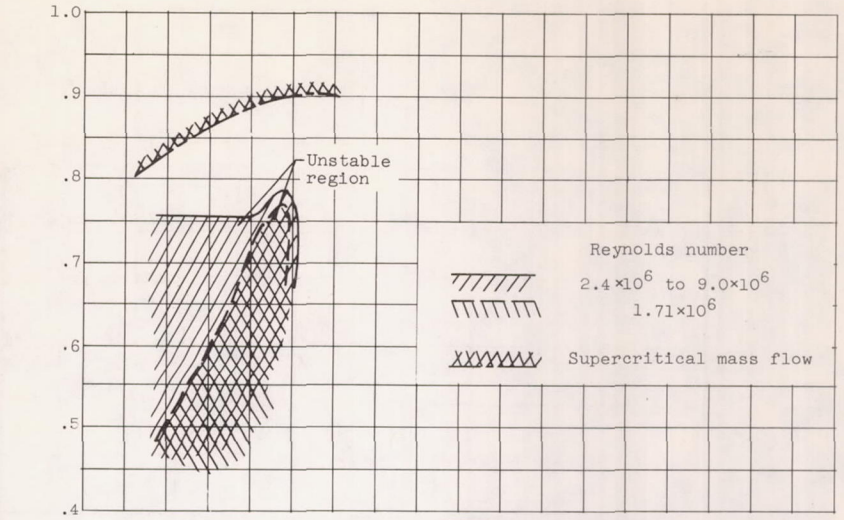
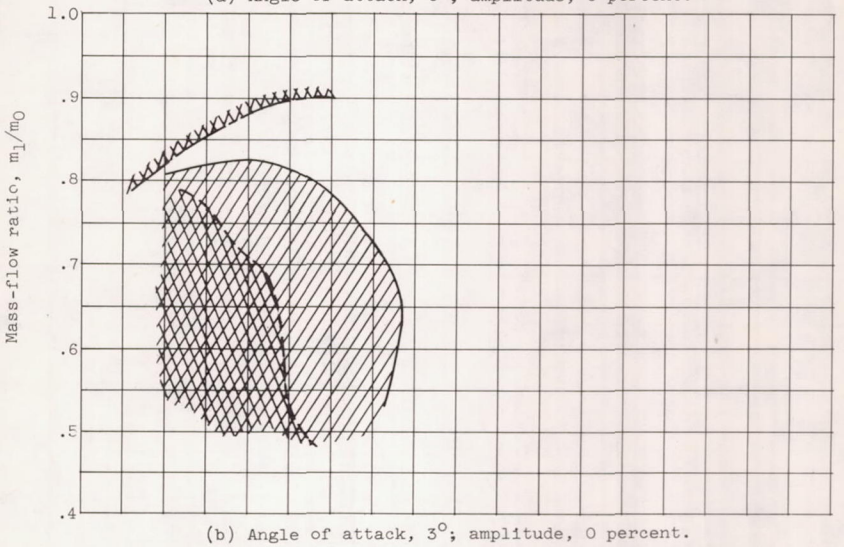


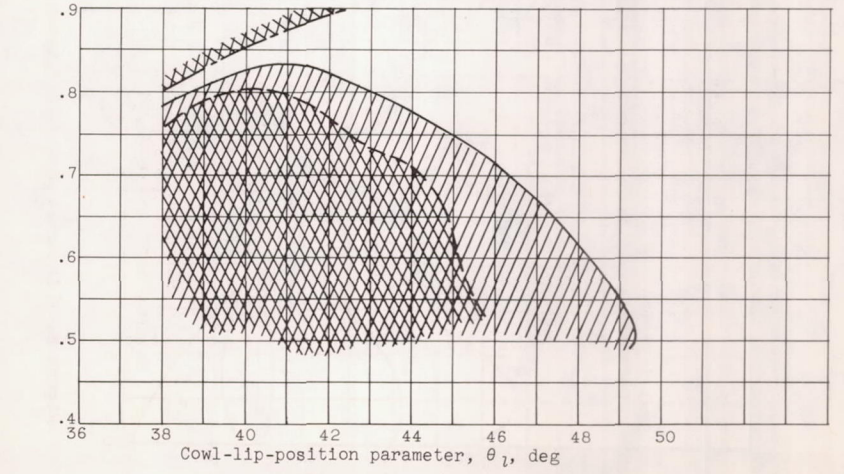

Figure 3. - Internal area distribution for various spike positions. (Nacelle station 0 located at vertical tangent to cowl lip.)




(a) Angle of attack, 0°; amplitude, 0 percent.




(b) Angle of attack, 3°; amplitude, 0 percent.




(c) Angle of attack, 6°; amplitude, 5 percent.

Figure 4. - Effect of Reynolds number on stability limits for cold pipe.

[redacted]

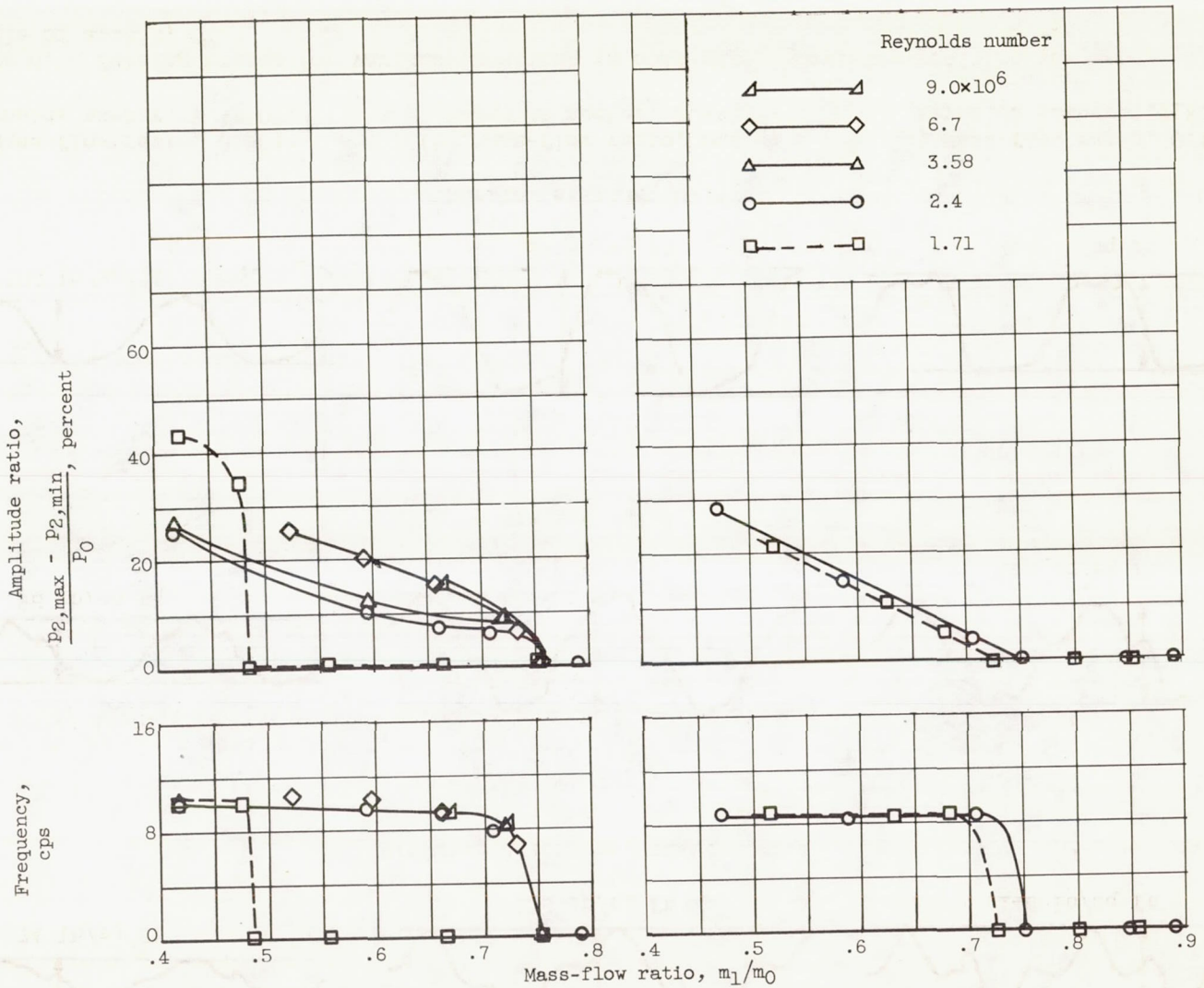
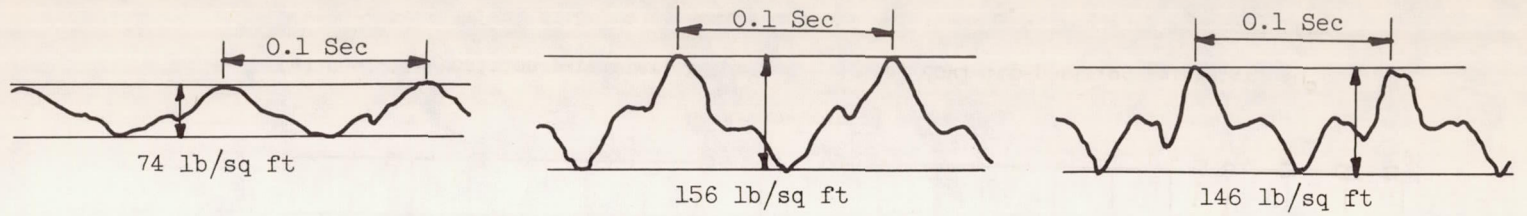
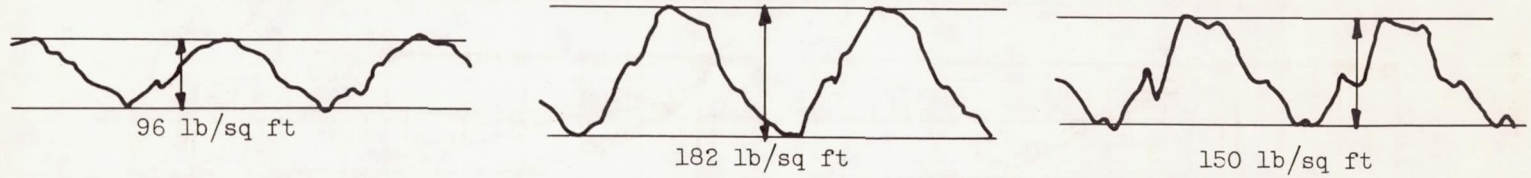


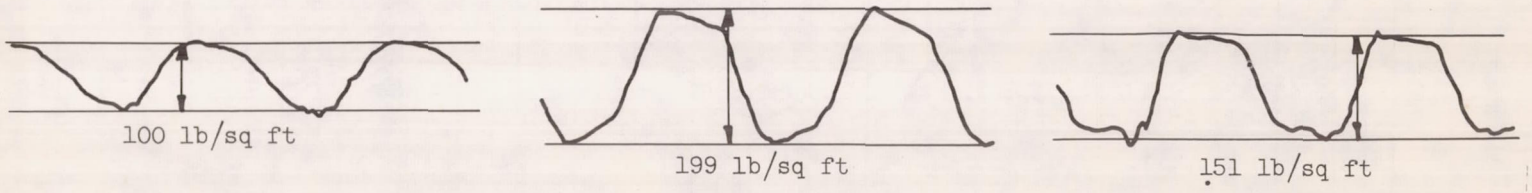

Figure 5. - Effect of Reynolds number on buzz amplitude and frequency for cold pipe. Angle of attack, 0°.




Diffuser discharge, station 81.4




Station 157.4




Nozzle, station 207.4

(a) Mass-flow ratio, 0.59; Reynolds number, $2.4\times10^6$.

(b) Mass-flow ratio, 0.418; Reynolds number, $2.4\times10^6$.

(c) Mass-flow ratio, 0.45; Reynolds number $1.71\times10^6$.

Figure 6. - Pulsing traces for various locations in cold pipe. Cowl-lip-position parameter, $37.5^\circ$; angle of attack, $0^\circ$.

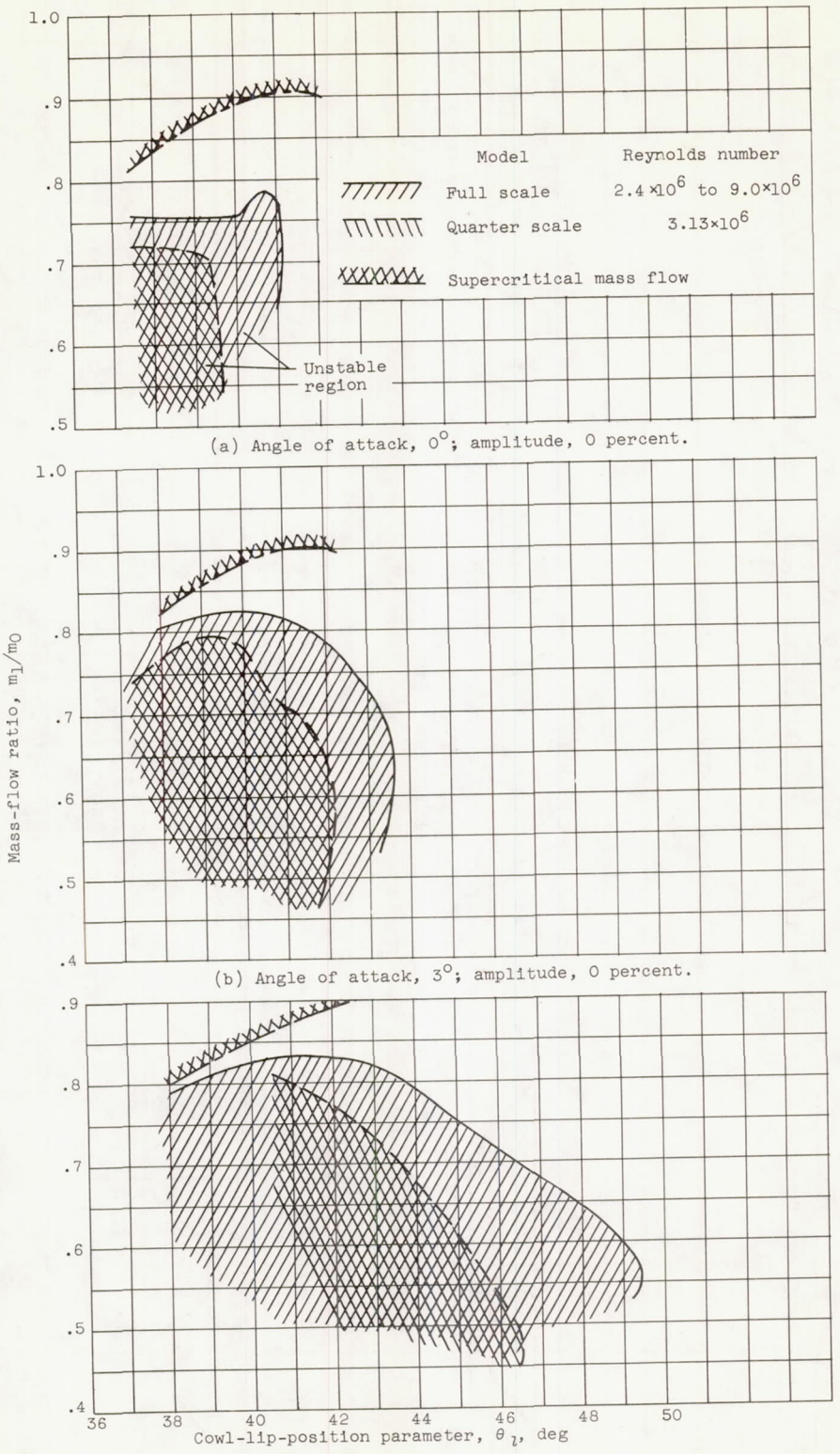



Figure 7. - Effect of model scale on stability limits for cold-pipe configurations.

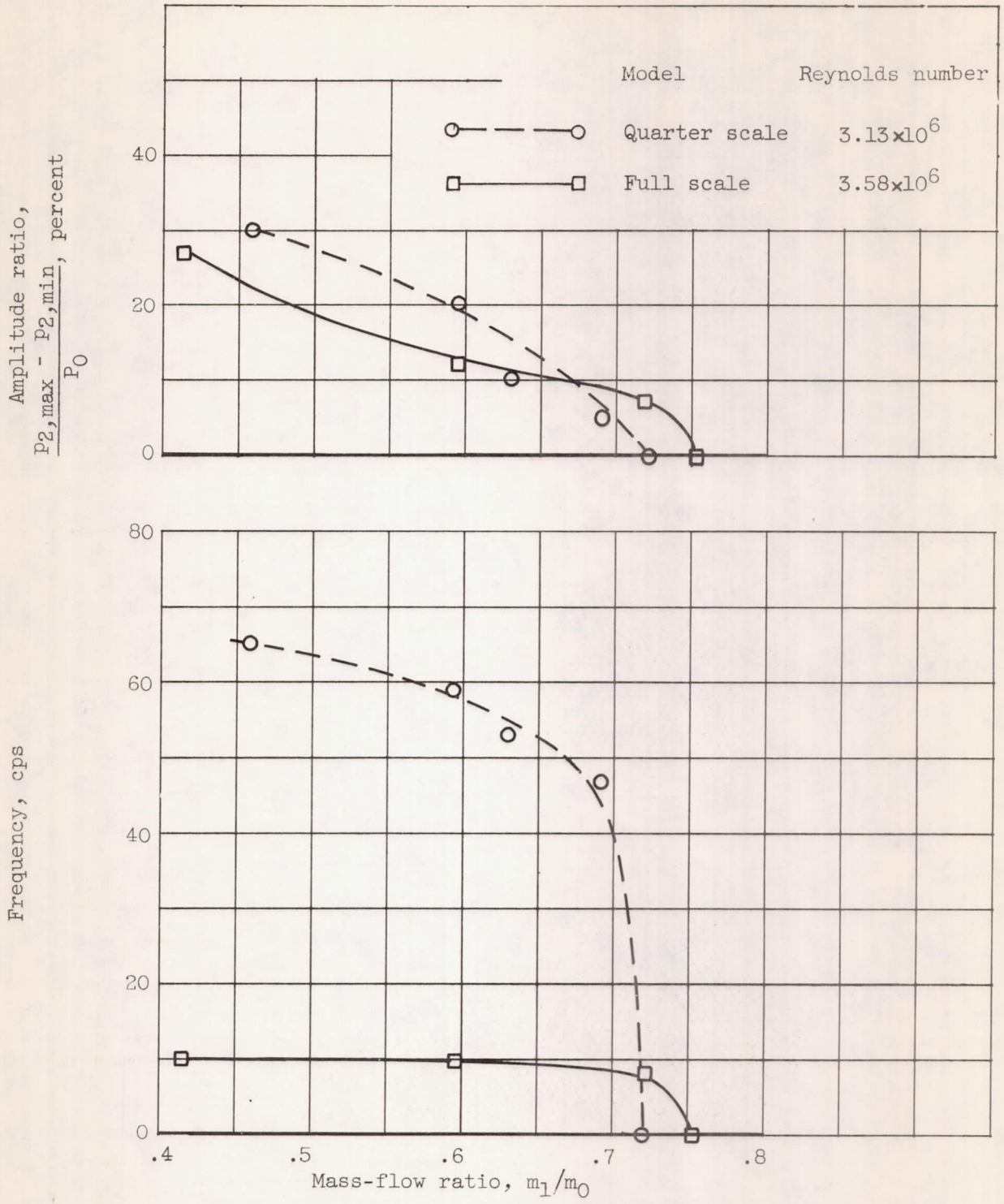
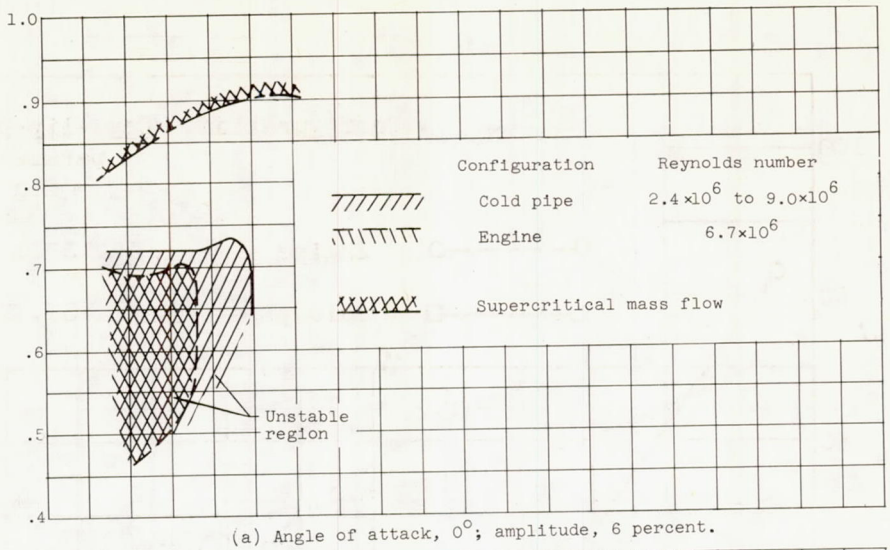
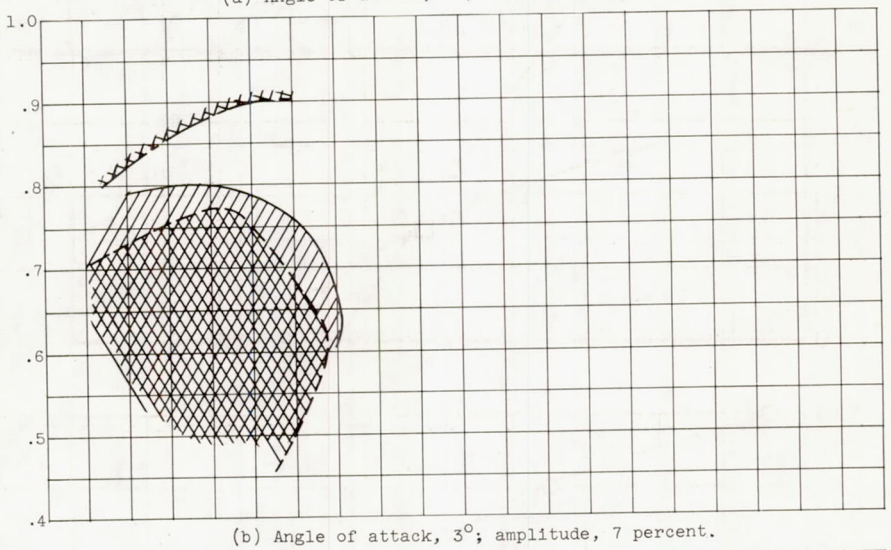


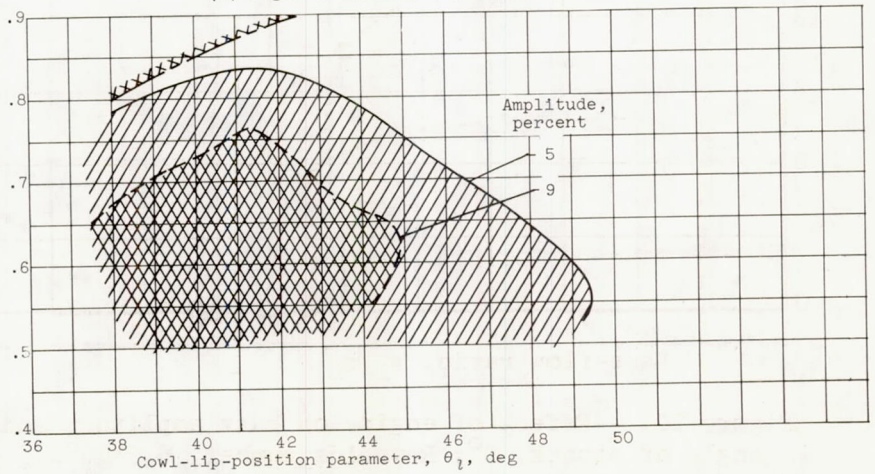

Figure 8. - Effect of model scale on buzz amplitude and frequency. Angle of attack, $0^{\circ}$; cowl-lip-position parameter, $37.75^{\circ}$.




(a) Angle of attack, 0°; amplitude, 6 percent.




(b) Angle of attack, 3°; amplitude, 7 percent.




(c) Angle of attack, 6°.

Figure 9. - Effect of engine on stability limits.

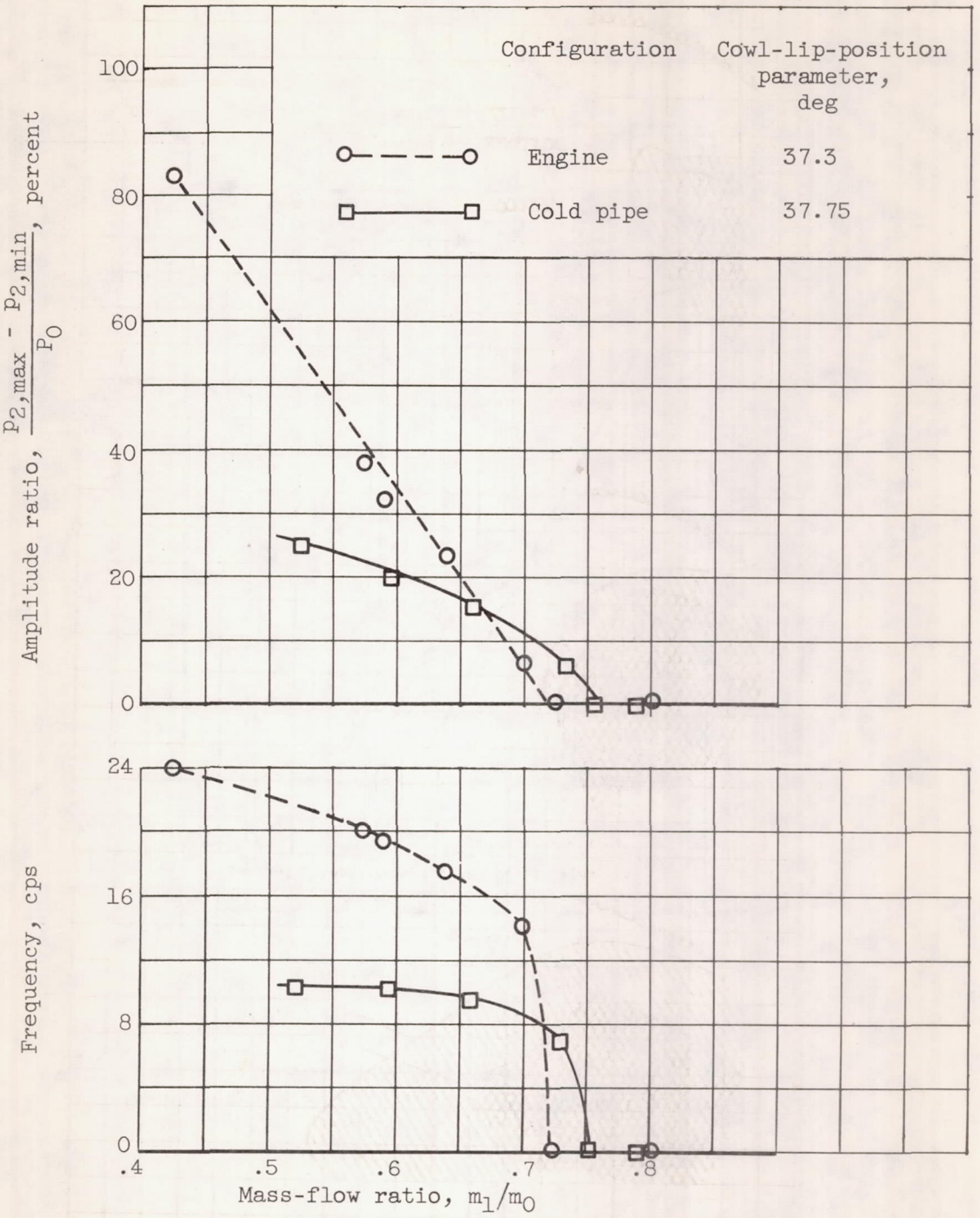
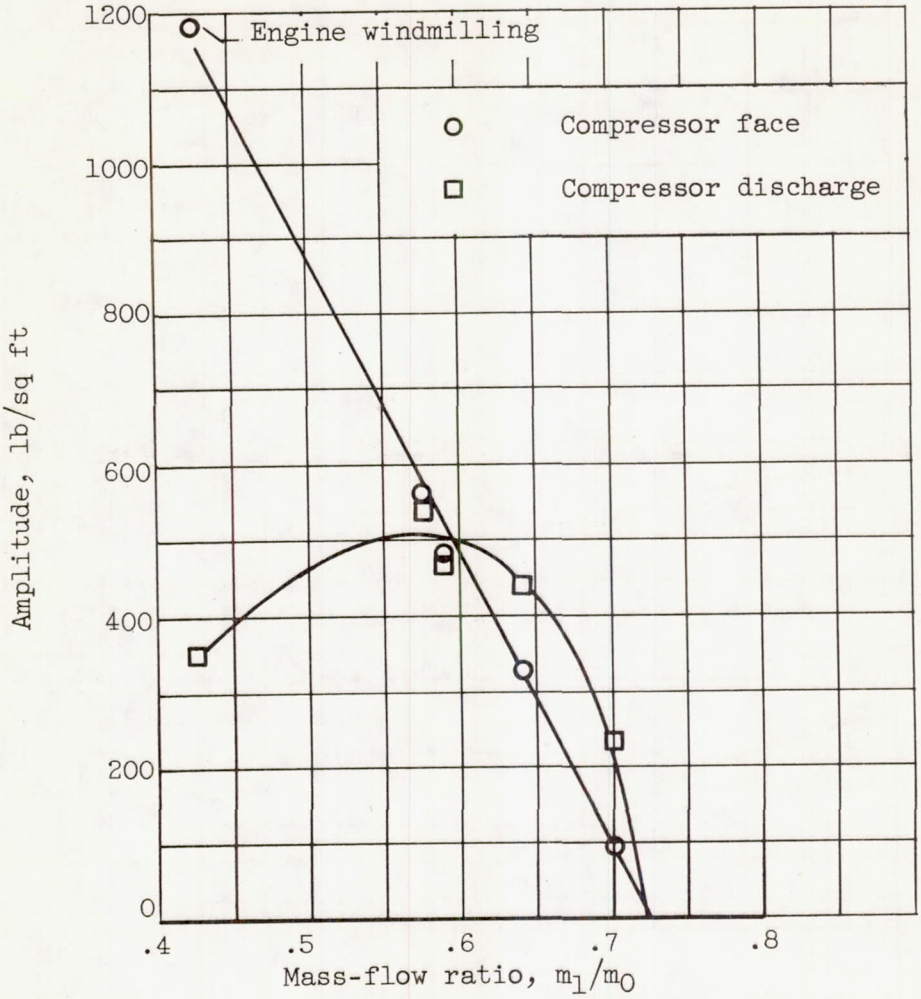


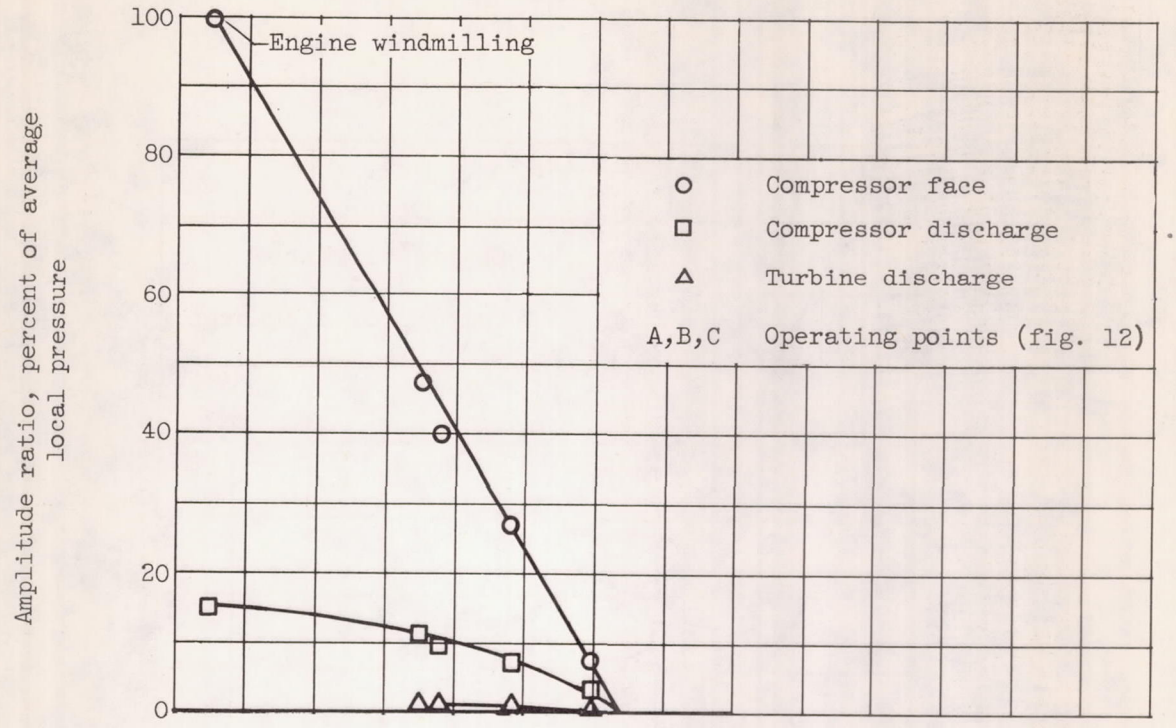

Figure 10. - Effect of engine on buzz amplitude and frequency. Angle of attack, $0^\circ$; Reynolds number, $6.7 \times 10^6$.

[redacted]

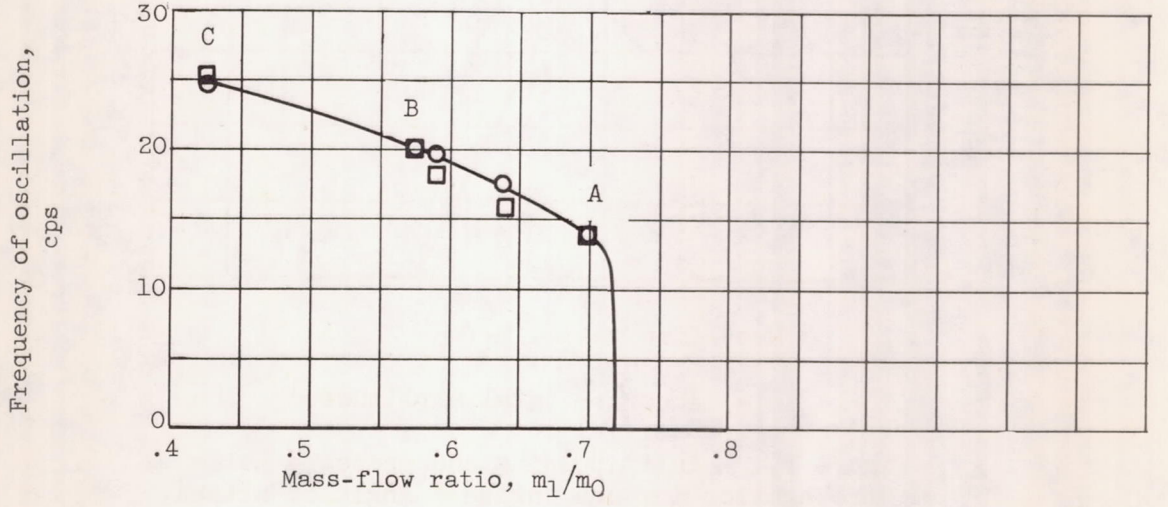



(a) Absolute total amplitude.

Figure 11. - Inlet pulsing and pressure pulse propagation through engine. Angle of attack, $0^\circ$; cowl-lip-position parameter, $37.3^\circ$.



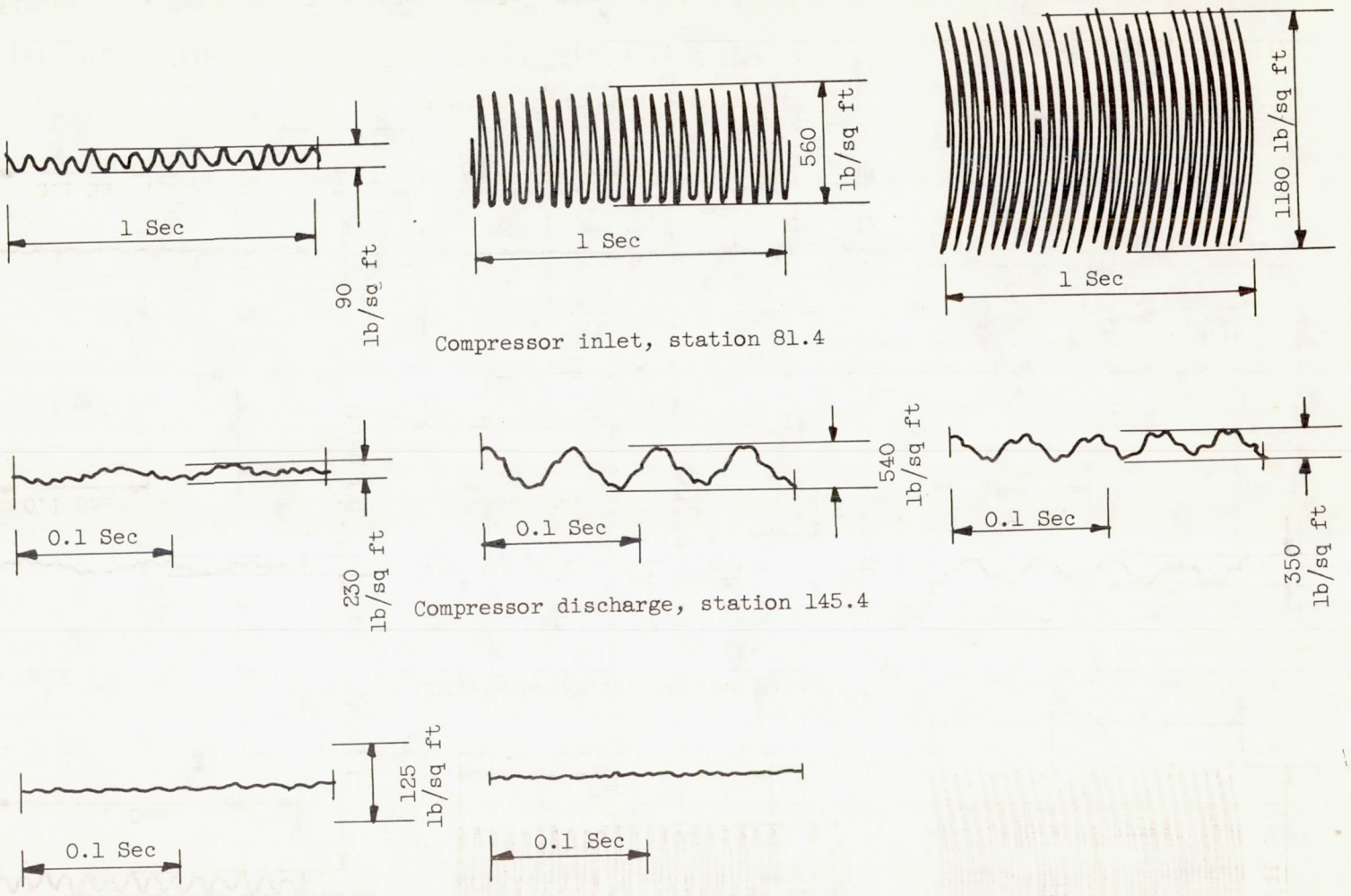

(b) Relative total amplitude.




(c) Frequency characteristics.

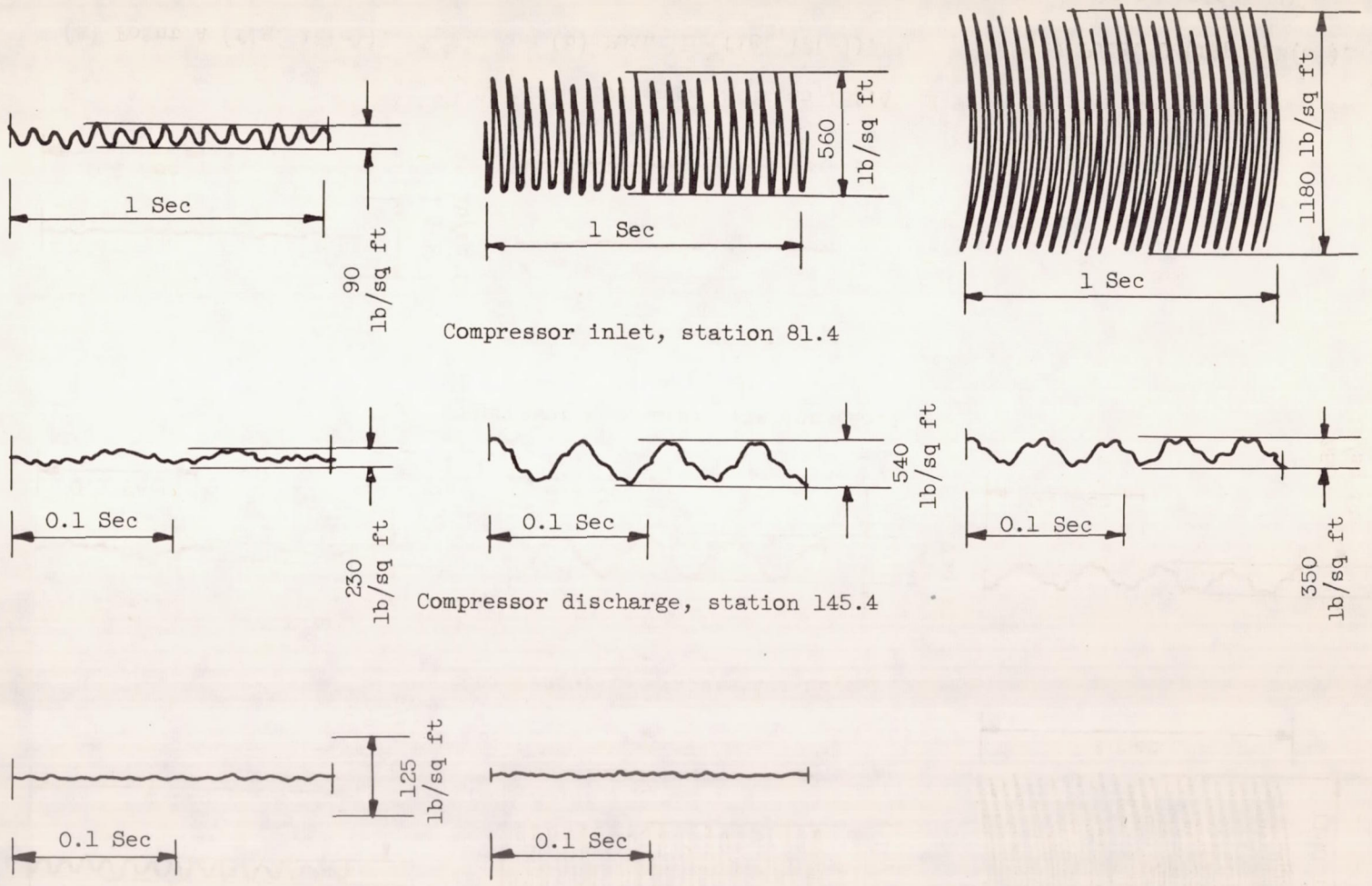
Figure 11. - Concluded. Inlet pulsing and pressure pulse propagation through engine. Angle of attack, $0^\circ$; cowl-lip-position parameter, $37.3^\circ$.

[redacted]




(a) Point A (fig. 12(c)). (b) Point B (fig. 12(c)). (c) Point C (fig. 12(c)).

Figure 12. - Examples of pressure traces during inlet pulsing with engine. Angle of attack, $0^{\circ}$.

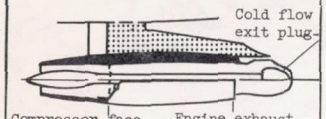
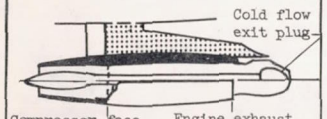
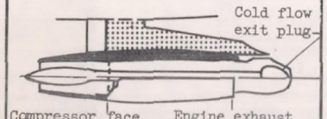
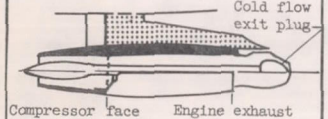



(a) Point A (fig. 12(c)). (b) Point B (fig. 12(c)). (c) Point C (fig. 12(c)).

Figure 12. - Examples of pressure traces during inlet pulsing with engine. Angle of attack, $0^{\circ}$.

NOTES: (1) Reynolds number is based on the diameter of a circle with the same area as that of the capture area of the inlet.

(2) The symbol * denotes the occurrence of buzz.

| Report and facility | Description | | | Test parameters | | | | Test data | | | | Performance | | Remarks |
|---|---|---|---|---|---|---|---|---|---|---|---|---|---|---|
| | Configuration | Number of oblique shocks | Type of boundary-layer control | Free-stream Mach number | Reynolds number $\times 10^{-6}$ | Angle of attack, deg | Angle of yaw, deg | Drag | Inlet-flow profile | Discharge-flow profile | Flow picture | Maximum total-pressure recovery | Mass-flow ratio | |
| CONFID. RM E57D17 Lewis 10-by 10-ft unitary wind tunnel |  Full-scale nacelle | 1 | None | 2.0 | 1.74 to 9.2 | 0,3,6 | 0 | | | | | 0.9 | (0.425 - 0.90)* | An investigation of the stability of a full-scale, blunt-lip cowl with an engine and with an exit plug was made. Full-scale inlet - exit-plug stability characteristics were compared to those of a quarter-scale inlet. The effect of Reynolds number on the full-scale-inlet - exit-plug stability characteristics was determined. |
| CONFID. RM E57D17 Lewis 10-by 10-ft unitary wind tunnel |  Full-scale nacelle | 1 | None | 2.0 | 1.74 to 9.2 | 0,3,6 | 0 | | | | | 0.9 | (0.425 - 0.90)* | An investigation of the stability of a full-scale, blunt-lip cowl with an engine and with an exit plug was made. Full-scale inlet - exit-plug stability characteristics were compared to those of a quarter-scale inlet. The effect of Reynolds number on the full-scale-inlet - exit-plug stability characteristics was determined. |
| CONFID. RM E57D17 Lewis 10-by 10-ft unitary wind tunnel |  Full-scale nacelle | 1 | None | 2.0 | 1.74 to 9.2 | 0,3,6 | 0 | | | | | 0.9 | (0.425 - 0.90)* | An investigation of the stability of a full-scale, blunt-lip cowl with an engine and with an exit plug was made. Full-scale inlet - exit-plug stability characteristics were compared to those of a quarter-scale inlet. The effect of Reynolds number on the full-scale-inlet - exit-plug stability characteristics was determined. |
| CONFID. RM E57D17 Lewis 10-by 10-ft unitary wind tunnel |  Full-scale nacelle | 1 | None | 2.0 | 1.74 to 9.2 | 0,3,6 | 0 | | | | | 0.9 | (0.425 - 0.90)* | An investigation of the stability of a full-scale, blunt-lip cowl with an engine and with an exit plug was made. Full-scale inlet - exit-plug stability characteristics were compared to those of a quarter-scale inlet. The effect of Reynolds number on the full-scale-inlet - exit-plug stability characteristics was determined. |

Bibliography

These strips are provided for the convenience of the reader and can be removed from this report to compile a bibliography of NACA inlet reports. This page is being added only to inlet reports and is on a trial basis.